03

Wave front reconstruction based on the photometric and interference measurements

© G.G. Levin[1], V.L. Minaev[1], A.A. Samoilenko[1,¶], T.V. Yakovleva[2]

[1] All-Russian Research Institute for Optical and Physical Measurements,
119361 Moscow, Russia
[2] Federal Research Center „for Informatics and Management, " Russian Academy of Sciences
119333 Moscow, Russia
]1mm ¶e-mail: asamoylenko@vniiofi.ru

Received December 05, 2022
Revised December 05, 2022
Accepted January 10, 2023

The paper presents a new original technique for accurate reconstructing the wave front phase at interferometry measurements based upon the estimation of the signals? amplitudes. The optical signals? processing is implemented within the Rice statistical model. The required phase of the wave front to be reconstructed is calculated from the geometrical considerations from the calculated undistorted amplitudes values. The paper provides both the mathematical basics of the technique and the results of its testing by means of both numerical and physical experiments. The proposed technique can be efficiently applied in a wide circle of scientific and technical tasks in numerous ranging and communication systems.

Keywords::

DOI: 10.61011/EOS.2023.02.55798.4412-22

Introduction

Reduction of the phase of optical radiation that has passed through or reflected from an object has always played an important role in optical measurements. This led to the widespread use of interferometry methods and the appearance of a large number of interferometers of various types. The key link in these devices is the deciphering of interference patterns, i. e. reduction of the phase distribution of the wave front, which carries information about the studied object. Very significant results have been obtained along the way.

The most common way to reconstruct the phase from interference measurements is a group of phase stepping methods, which is based on recording several interference patterns of the same object with a deterministic retardance in the reference channel and the subsequent joint processing of the obtained interference patterns.

The specific feature of the phase-step methods is the requirement of careful calibration of the retardance value in the reference channel, which leads to changes in the interference fringes, because its value is embedded in the calculated formulas for the phase [1].

At present, the so-called self-calibrating algorithms have appeared, in which the retardance value is determined by interference patterns [2–6]. As a rule, this requires the presence of some number of fringes — interference patterns with the carrier. However, in some cases, obtaining interference patterns without a carrier is the only possible or more preferable option. For example, sometimes when using low-coherence sources, it is difficult to obtain interference patterns on the carrier, and in the Fizeau interferometer scheme, when studying large optical parts, it is desirable that the beams follow the same path, and therefore, the interference patterns were also without carrier. When the retardance device is calibrated, an artifact occurs in the form of „second harmonic" — phase modulation, repeating the interference fringes, but of double frequency [7]. Therefore, the actual task is to develop a phase step method independent of the retardance device calibration and capable of operating with a small number of interference fringes.

The aim of this work is to analyze an algorithm for reconstructing the phase distribution based on the joint processing of photometric and interference data without using a deterministic retardance device.

Theoretical foundations

Let us consider the process of object field interference

$$E_0(x,y) = A(x,y)\exp[-ik\varphi(x,y)],$$

where $k = 2\pi/\lambda$, and the reference field

$$E_r(x,y) = B(x,y)\exp[-ik\phi(x,y)]$$

assuming their partial coherence with the spatial distribution of the coherence function $\gamma(x,y)$ [8]. Then, the canonical equation of the interference pattern has the form

$$I(x,y) = A^2(x,y) + B^2(x,y) + 2A(x,y)B(x,y) \times \cos\big[k\big(\varphi(x,y) - \phi(x,y)\big)\big]\gamma(x,y), \qquad (1)$$

where $\gamma(x, y)$ — the coherence function in the interference pattern registration plane determining the contrast of fringes.

From expression (1)b it is not difficult to obtain the following expression for the phase difference of the desired wave front and the known phase distribution of the reference wave:

$$\varphi(x, y) - \phi(x, y) = (1/k)\arccos\big[\big(I(x, y) - A^2(x, y) - B^2(x, y)\big)/\big(2A(x, y)B(x, y)\gamma(x, y)\big)\big]. \quad (2)$$

It is easy to see that for the phase reduction, it is necessary to solve several problems: measure the intensity distribution $A^2(x, y)$, $B^2(x, y)$ and $I(x, y)$, to measure the coherence function in the interference pattern formation plane, to calculate the arccos function for different arguments.

Let us elaborate on the solution to each problem.

Measuring the intensity distribution

It is obvious from expression (2), that errors in determining the distribution of radiation intensities in each channel significantly affect the phase reduction, since the arccos function is significantly nonlinear for argument values close to 1. In order to determine this effect, we conduct a numerical simulation of the algorithm under noise conditions.

The process of formation of the „slow" component fields E_o and E_r in each channel of the interferometer in the presence of noise can be written in the form of

$$R_{o,r} = E_{o,r} + n\exp(i\varphi),$$

where E — the non-noise (true) value of the signal. The value E is complex, which allows to consider the wave phase in the simulation of optical measurements, n — a real random variable whose value obeys the Rayleigh distribution with a scale parameter σ, ϕ random phase, which has a uniform distribution in the range from 0 to 2π, indices o, r refer to the object and reference waves, respectively. The complex value R has been used for various calculations, in which not only the amplitude but also the phase of the wave matters, for example, to calculate the interference pattern of two waves. To calculate the amplitude r distribution in each channel from R, a modulus was taken:

$$r = |R|.$$

To compensate for the noise effect on the intensity distribution measurements in each channel and interference pattern, it is necessary to perform averaging over realizations. When using statistical methods of signal processing, the specific features of the distribution to which the analyzed data are subject are essential.

It is known that the amplitude of the signal formed as a result of Gaussian noise on an initially deterministic signal is a random variable, which obeys the statistical distribution of Rice [9].

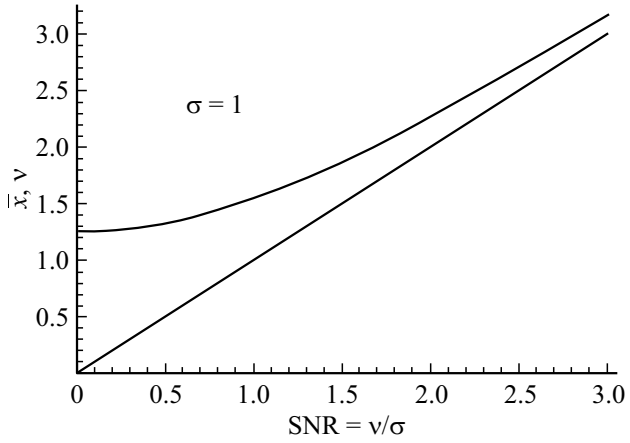

Figure 1. Illustration of the mismatch between the average Rice signal $\overline{x}$ and the Rice parameter ν as a function of the signal-to-noise ratio, $SNR = \nu/\sigma$.

In Rice signal analysis problems, the measured quantity is the amplitude $x = \sqrt{x_{\mathrm{Re}}^2 + x_{\mathrm{Im}}^2}$ of a complex variable with real x_{Re} and imaginary x_{Im} components, characterized by its mean value and distorted by a normally distributed Gaussian noise with variance σ^2. These conditions characterize many tasks of signal processing of different physical nature. The amplitude $x = \sqrt{x_{\mathrm{Re}}^2 + x_{\mathrm{Im}}^2}$ obeys a Rice distribution with a probability density function

$$P\left(x|\nu, \sigma^2\right) = \frac{x}{\sigma^2}\exp\left(-\frac{x^2 + \nu^2}{2\sigma^2}\right)I_0\left(\frac{x\nu}{\sigma^2}\right),$$

where $I_\alpha(z)$ — modified Bessel function of order one α. The problem to be solved is to determine the unknown parameters ν and σ^2 on the basis of the data obtained from measurements.

Because of the specific features of the Rice statistical distribution, the Rice data analysis requires the development of specific methods and appropriate mathematical apparatus. It is known that when processing Gaussian data, the traditional means of filtering is data averaging. However, as noted above, unlike the Gaussian distribution case, the average value of the Rice signal $\overline{x}$ is not the same as the desired value of the useful signal ν. This is shown in Fig. 1, where the mean value of the Rice signal $\overline{x}$ is represented by a curved line, and the true value of the signal is represented by a straight line coming from the origin. The average value of the Rice signal as a function of Rice parameters is expressed by the following formula:

$$\overline{x} = \sigma\sqrt{\pi/2}I_{1/2}(-\nu^2/2\sigma^2).$$

In (2) $L_{1/2}(z)$ — the Laguerre polynomial.

The graphs in Fig. 1 correspond to fixed values of the noise parameter σ: $\sigma = 1$, so the values on the abscissa axis correspond to the signal-to-noise ratio.

Thus, if traditional averaging filtering methods are applied to data subject to Rice statistics, the true signal values are distorted in the area of small signal-to-noise ratio values.

The presence of such an error in the averaging of Rice data is strictly justified in works [10–16]. The presence of an unavoidable error means that simple averaging is inapplicable to correctly solve the problem and the need to use data processing methods that take into account the specific features of the Rice statistical model.

In [10–16], an exact theory of statistical processing of Rice signals was developed and new mathematical methods for the so-called two-parameter approach to Rice data analysis were rigorously justified. This approach involves solving the problem of Rice data analysis by jointly estimating signal and noise.

The specific theoretical methods developed as part of the two-parameter Rice signal analysis in [14–16] differ in the basic statistical principles on which they are based. One such theoretical technique involves the method of moments. This technique is based on the processing of measured data for 2nd and 4th moments and is designated as M24.

The solution to the two-parameter Rice signal analysis problem by the MM24 method is based on the known formulas for the 2nd and 4th initial moments of the Rice random variable [17]:

$$\begin{cases} \overline{x^2} = 2\sigma^2 + \nu^2, \\ \overline{x^4} = 8\sigma^4 + 8\sigma^2\nu^2 + \nu^4. \end{cases} \tag{3}$$

Considering formulas (3) as a system of two equations for the two unknown variables A and σ^2, we can calculate the required values ν and σ^2 based on data for the second $\overline{x^2}$ and the fourth $\overline{x^4}$ moments of Rice value x obtained from sample measurements [16,18].

From the formulas (3), to determine the required Rice parameters A and σ^2, it is not difficult to obtain the following expressions:

$$A^2 = \overline{x^2}\sqrt{1-t},$$

$$\sigma^2 = \frac{\overline{x^2}}{2}\left(1-\sqrt{1-t}\right). \tag{4}$$

In expressions (4), the notation was introduced

$$t = \frac{\overline{x^4}}{\left(\overline{x^2}\right)^2} - 1.$$

It is easy to see that for any random variable x, due to the stochasticity of the variable x^2, the condition $\overline{x^4} - \left(\overline{x^2}\right)^2 > 0$ is satisfied, since the difference $\overline{x^4} - \left(\overline{x^2}\right)^2$ determines the variance of the random variable x^2. Therefore, the entered parameter t grows with the process stochasticity and satisfies the relation $0 < t \leq 1$. The limiting case $t = 1$ corresponds to a particular case of the Rice — Rayleigh distribution, when there is noise and no useful signal ($A = 0$).

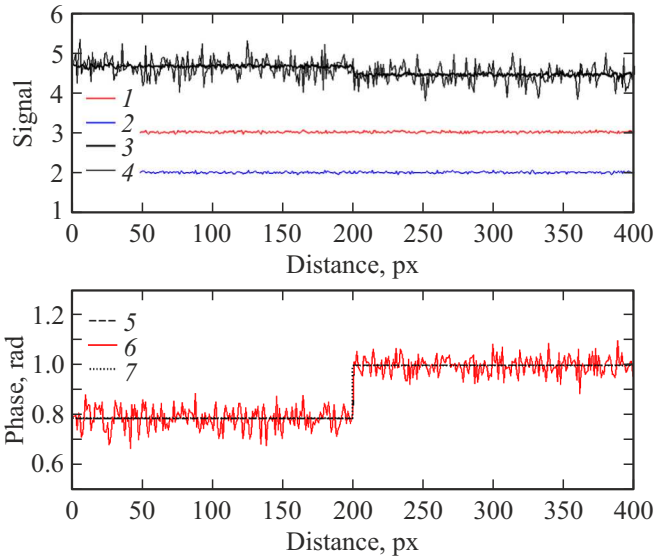

Figure 2. Simulation of phase step profile reduction using the MM24 method for processing interference and photometric measurements. *1* — object wave, averaged; *2* — support wave, averaged; *3* — interference wave, averaged; *4* — interference wave, single realization; *5* — value; *6* — signal reduced by Rice; *7* — average signal level by Rice.

Thus, the MM24 method makes it possible to jointly calculate by formulas (4) both the desired estimation of signal value A and noise variance σ^2, which is important for subsequent image processing.

The efficiency of statistical data analysis by the MM24 method for optical phase measurements is substantiated, in particular, in work [19].

Results of numerical experiments

Using the MM24 method to process the interference and photometric measurements, we simulated the reduction of the phase step profile. The reduction results are shown in Fig. 2. The upper graph shows the results of measurements separately for the object wave, separately for the reference wave and the result of their interference. Wherein,

- the true value of the object wave had an amplitude of 3 (in conditional units) and a phase of $\phi_{ob} = \pi/4$ from the 1st to the 200th pixel, and from the 201th to the 400th pixel, the phase was $\phi_{ob} + \phi_h$, where ϕ_h — the height of the phase step, corresponding to 20 nm at a wavelength of 600 nm;
- the true value of the reference wave had all amplitude 2 and phase 0;
- the interference wave was the sum of the noisy object and reference waves;
- the noise level for the object and reference waves was the same and was $\sigma = 1$;
- averaging for the interference pattern was performed for 256 realizations. For the object and reference waves, averaging was performed over 256 random samples of the

same realization, since the desired field amplitude was the same everywhere. In a real experiment, as a rule, the interferometer is adjusted so that the field amplitudes in the reference and signal channels are the same and uniform throughout the instrument field of view, so this procedure is also possible.

The bottom graph shows the results of phase step reduction from measurements averaged using the M24 method.

Phase reduction using conventional averaging results not only in a shift of the entire phase front, but also in a phase change that depends on the noise level and its value proper.

Fig. 3 shows the results of the simulation of the phase step reduction at different values of the noise parameter σ. The step height 20 nm. Number of implementations 1000. Other parameters are the same. The upper graph shows the dependencies of the reduction upper and lower step levels on the noise level. The bottom graph shows the dependence of the step height estimate divided by its true height, also from the noise level on the measured data. The graphs show that, unlike the MM24 method, the estimation by conventional averaging gives distorted values. However, when the signal-to-noise ratio is small, the reduction error increases when using the MM24 method. This is due to the fact that starting $\sigma \approx 1.5$ in this method, there are negative values below the root in the expression (4) for some points in the formulas. Such points were excluded from the averaging, which led to distortions.

Thus, averaging the experimental data using Rice statistics makes it possible to recover the true value of the field phase from the photometric and interference data at any signal-to-noise ratio.

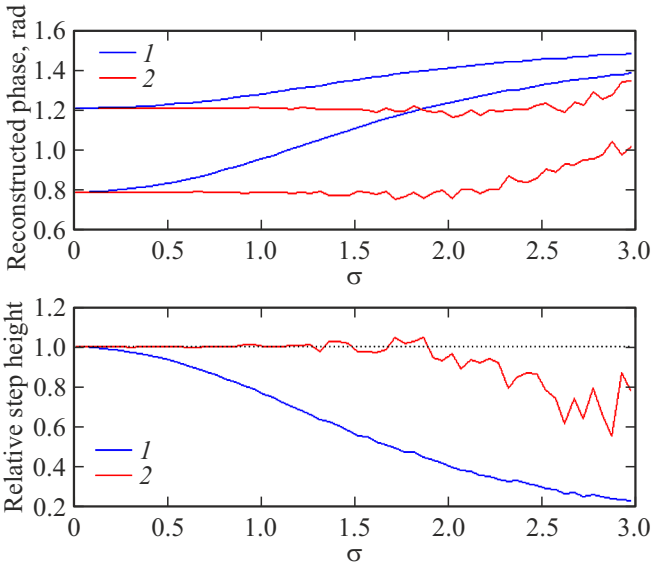

Figure 3. Simulation results for phase step reduction at different values of the noise parameter. *1* — simple averaging, *2* — Rice averaging.

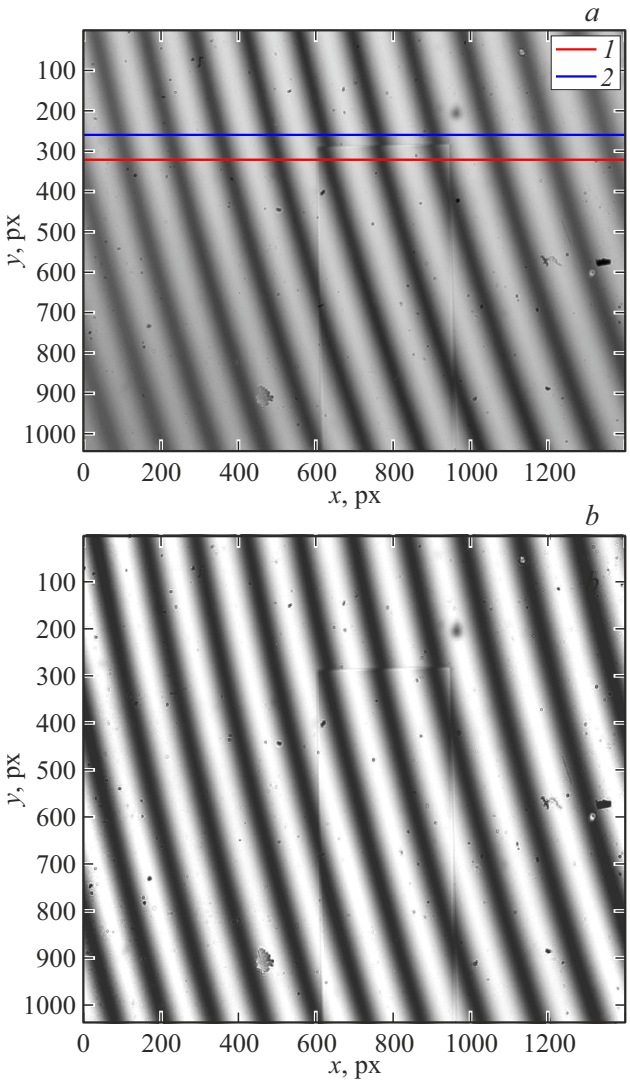

Figure 4. Interference pattern obtained with an interference microscope (*a*); same interference pattern normalized to the coherence function (*b*). *1* — step , *2* — base .

Measuring the distribution of the coherence function by species of the bands on the interference pattern

The second factor affecting the phase measurement accuracy with the proposed method is the spatial heterogeneity of the coherence function in the area of interference pattern formation. This is due to the fact that modern interferometers use radiation sources with partial coherence. Fig. 4, *a* shows an interference pattern obtained with an interference microscope with a low-coherence source [1]. An LED (model M530L3 from ThorLabs) with a wavelength of 530 nm was used as a light source in the microscope. As you can see from the figure, the visibility of the fringes varies by image field. Consequently, it is necessary to determine the coherence coefficient, which will be different at different points of the interference pattern. To compensate

for the influence of non-uniformity of fringe contrast, a two-step procedure was developed to determine the distribution of the coherence function over the image field, based on the processing of a flat surface interference pattern. At the first stage, sets of local maxima and minima were determined in each line of the image. The maxima and minima were approximated by two-dimensional fourth-order polynomials. In the result, two smooth surfaces enveloping the interference pattern from above and below were obtained. Next, the interference pattern was normalized using these two surfaces so that the minimum corresponds to a value of -1, and the maximum — $+1$.

At the second stage of normalization, we used cubic splines drawn along the maxima and minima. To reduce the noise effect on the result, these lines were first passed through a low-pass filter. This procedure made it possible to almost completely eliminate the coherence function non-uniformity over the entire field of view of the interferometer. Fig. 4, *b* shows an interference pattern normalized to the coherence function. Thus, the use of the proposed algorithm requires a preliminary measurement of such a characteristic as the coherence function distribution of the coherence function in the interference pattern registration plane.

Field phase calculation

According to expression (2), in order to calculate the phase, it is necessary to calculate the arccos function from the values obtained after processing the photometric and interference data. This function is defined in the range from -1 to 1 and is linear for values of the argument around zero. However, when approaching the range boundaries, its derivative tends to infinity. Therefore, in the presence of noise, there is a significant amplification of the noise of the reduction phase at values of the argument close to ± 1. In the present work, to compensate for this effect, another interference pattern with a retardance of the reference channel of about a quarter of a wavelength is proposed. In this case, the part of the phase distribution where the arccos argument of the first interference pattern has values around zero will be reduced from the first interference pattern, and the other part of the distribution — from the second interference pattern. It is easy to see that it is not necessary to know the retardance value in the reference channel, as it is easily calculated from the phase difference in the overlapping areas of the argument.

Experimental findings

To verify the proposed method, a physical experiment was carried out to reduce the step shape of the SHS−180 QC measure produced by VLSI Standards Inc. Certified step height 19.9 ± 0.8 nm. The measurements were made with a low-coherence source [1] interference microscope. This microscope has a Linnik circuit with a reference mirror mounted on a piezo element. Thus, it is possible to set the desired offset of the reference mirror.

The microscope was used to obtain an interference pattern between the images of the step and the reference mirror (interference pattern), an image of the step without interference (with overlapped reference channel) and an image of the reference mirror (with overlapped object channel). Images of each type were obtained by a series of 9 images followed by averaging using the MM24 method. In addition, two fringe pattern were obtained that differ from each other in the phase of the interference fringes by approximately $\pi/2$.

An LED (model M530L3 from ThorLabs) with a wavelength of 530 nm was used as a light source in the microscope.

An example of the resulting interference pattern is shown in Fig.4. As can be seen from the figure, due to the unevenness of the coherence function, the contrast of the fringes varies across the image field. The coherence function distribution over the image field was preliminarily determined according to the above technique. The phase distribution was calculated along two lines, one of which crossed the step, and the other passed outside of it. This is necessary in order to determine the baseline characterizing optical aberrations and the general inclination of the plane.

The height from the phase overrun in length units was recalculated by the formula

$$h_{nm} = \frac{h_{\text{rad}}}{4\pi}\,\lambda,$$

where λ — the wavelength of the LED 530 nm, and 4 instead of 2 is because the light makes two passes when the image is acquired.

Subtracting the base from the step results in a visually straight step. According to the methodology used to calibrate the ZYGO [20] profilometer, to calculate the step height, it is necessary to calculate the average height of two sections on different sides of the step, as well as the average height of the profile section that is on the step, while you need to step back from its edge, as there are sharp phase jumps due to diffraction at the edge. The step height will be the difference of these two values.

Since the slope was subtracted from the profiles reduction (each profile has its own slope), the resulting step also has a slight slope. To eliminate the effect of this slope on the result, the areas for averaging on the base were taken symmetrical about the area on the step so that the „center of mass“ of the substrate areas is under the „center of mass“ of the step area.

The step with the subtracted base and the result of the step height measurement are shown in Fig. 5. The averaging areas are highlighted in red and green, and the dashed line shows the calculated step height. The measured step height was 19.29 nm, which agrees well with its certified height of 19.9 ± 0.8 nm.

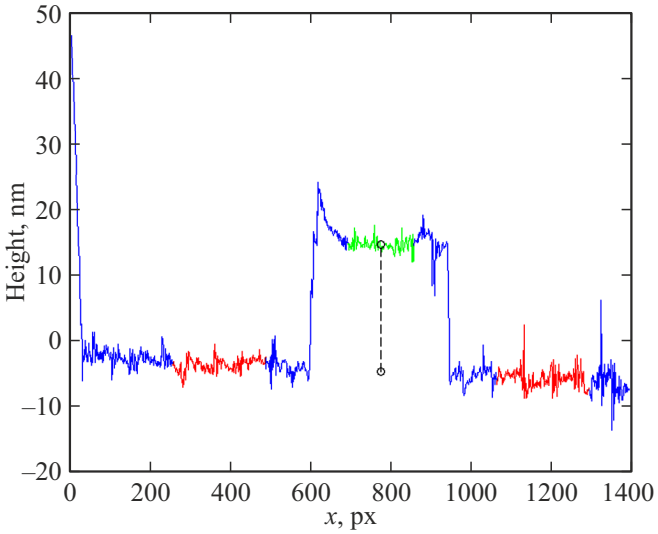

Figure 5. Reduced step profile with subtracted base and height measurement result

.

Conclusions

Mathematical modeling and experimental results show that the joint processing of photometric and interference measurements using the algorithm proposed in this work allows us to reduce the phase distribution with sufficiently high accuracy, even in the presence of noise. In this case, the requirements to the retardance device are significantly reduced. However, there are serious requirements for pre-calibration of the interferometer according to the spatial distribution of the coherence function. Another requirement of the proposed algorithm is the uniformity of intensity distribution in the reference and signal channels of the interferometer. This greatly simplifies the processing of photometric data, because it allows to use Rice methods of data analysis of averaging the distributions of the amplitudes of the object and reference channels on a single frame at random sampling counts.

References

[1] V. Minaev, G. Vishnyakov, G. Levin. Instruments and Experimental Techniques, **61** (6), 856 (2018). DOI: 10.1134/S0020441218060210
[2] K. Larkin. Optics Express, **9** (5), 236 (2001). DOI: 10.1364/OE.9.000236
[3] H. Du, J. Yan, J. Wang. Appl. Optics, **56** (11), 3071 (2017). DOI: 10.1364/AO.56.003071
[4] K. Yatabe, K. Ishikawa, Y. Oikawa. J. Opt. Soc. Am. A, **34** (1), 87 (2017). DOI: 10.1364/JOSAA.34.000087
[5] H. Guo, Z. Zhang. Appl. Optics, **52** (26), 6572 (2013). DOI: 10.1364/AO.52.006572
[6] G. Vishnyakov, G. Levin, V. Minaev, N. Nekrasov. Appl. Optics, **54** (15), 4797 (2015). DOI: 10.1364/AO.54.004797
[7] G.N. Vishnyakov, G.G. Levin, V.L. Minaev, I.Yu. Tsel'mina Opt. Spectrosc., **115**, 931–937 (2013). DOI: 10.1134/S0030400X13120217.
[8] M. Born, E. Volf. *Osnovy optiki* (Nauka, M., 1973) (in Russian)
[9] S.O. Rice. Bell Syst. Technological J., **23** (3), 282 (1944). DOI: 10.1002/j.1538-7305.1944.tb00874.x
[10] T.B. Yakovleva. *Teoriya obrabotki signalov v uslovitakh raspredeleniya Raysa* (In Russian) (A.A. Dorodnitsyn Computing Center of RAS, Moscow, 2015), p. 268.
[11] T. Yakovleva. J. Appl. Mathematics and Physics, **7** (11), 2767 (2019). DOI: 10.4236/jamp.2019.711190
[12] T.V. Yakovleva. Komp'yuternye issledovaniya i modelirovaniye, (in Russian) **8** (3), 445 (2016). DOI: 10.20537/2076-7633-2016-8-3-445-473
[13] T. Yakovleva. Appl. and Computational Mathematics, **7** (4), 188 (2018). DOI: 10.11648/j.acm.20180704.12
[14] T.V. Yakovleva. Computer Research and Modeling, **6** (1), 13 (2014). DOI: 10.20537/2076-7633-2014-6-1-13-25
[15] T.V. Yakovleva. Computer Research and Modeling, **6** (2), 231 (2014). DOI: 10.20537/2076-7633-2014-6-2-231-244
[16] T.V. Yakovleva, N.S. Kulberg. DAN, ser. Matematika, (in Russian). **459** (1), 27-31 (2014).
[17] J.H. Park, Jr. Q. Appl. Math., **19** (1), 45 (1961).
[18] T.V. Yakovleva, N.S. Kulberg. *Sposob dvukhparametricheskogo analiza sluchaynikh signalov na osnove izmerennykh dannikh dlya 2-go i 4-go momentov.* (In Russian) Invention patent №2556318 (2015).
[19] T.V. Yakovleva. Komp'yuternaya optika, **41** (6), 950 (2017). (in Russian). DOI: 10.18287/2412-6179-2017-41-6-950-956
[20] Zygo Corporation [Electronic resource]. URL: https://www.zygo.com/

Translated by Y.Deineka